The dielectric function and interband transitions in $Cd_{1-x}Zn_xTe$

1996 J. Phys.: Condens. Matter 8 5757

(http://iopscience.iop.org/0953-8984/8/31/009)

J. Phys.: Condens. Matter **8** (1996) 5757–5768. Printed in the UK

The dielectric function and interband transitions in $Cd_{1-x}Zn_xTe$

O Castaing†, R Granger†, J T Benhlal† and R Triboulet‡

† Laboratoire de Physique des Solides, ERS F0134 CNRS, INSA, F 35043 Rennes Cédex, France

‡ Laboratoire de Physique des Solides, LP 1332 CNRS, 1, place A Briand, F 92195 Meudon Cédex, France

Received 25 March 1996, in final form 22 April 1996

Abstract. Ellipsometric measurements of the dielectric functions of $Cd_{1-x}Zn_xTe$ solid solutions are given for the first time for the whole composition range at room temperature (293 K) between 0.75 eV and 5.7 eV. The energy and the broadening parameters for each critical transition are given as functions of the composition. The upward bowing of the energies is compared to theoretical estimates. The spin–orbit splittings in the valence band show a negligible bowing. Alloying leads to a small broadening which is negligible for the fundamental gap.

1. Introduction

$Cd_{1-x}Zn_xTe$ (CZTx) is now a leading material for epitaxial growth [1–3]. For instance it can be matched to HgCdTe for low x-values [4]. These solid solutions can be used in high-energy photon detectors [5] and also for bulk photorefractive devices when they are semi-insulating [6]. CZT are basic materials in heterostructures, leading to an enormous literature. CdTe/CdZnTe superlattices can block threading dislocation in heteroepitaxial growths [7]. These heterostructures have been thoroughly investigated, in the vicinity of the fundamental gap, mainly by optical techniques [8]. Recently these methods have allowed the characterization of the piezoelectric field in heterostructures grown along polar axes of the crystal [9].

The study of the optical properties of these solid solutions began in the seventies on bulk samples [10, 11, 12] and on thin films [13]. There are a great number of contradictions in the experimental results [14]. The variations of the energy of the critical transitions were found to be linear in x in [11] and [15] while they appear to be nonlinear in [10] and [12]. Moreover shoulders in the reflectivity and optical absorption curves have been attributed to transitions named e_1 and $e_1+\Delta_1$ below E_1 and $E_1+\Delta_1$, and two others around the transition named E_2 [10, 11, 13]. However e_1 and $e_1+\Delta_1$ were not evident in electroreflectance data [12].

As CZT became an important material its fundamental gap E_0 was measured at different temperatures and by several techniques [2, 16, 17]. There is also a relatively high discrepancy as regards the bowing parameter of E_0 [18] which increases from 0.139 eV as measured for epitaxial layers [16] to 0.32 eV as measured using photoreflectance for bulk materials [2]. Very recently the dielectric function has been deduced from spectroscopic ellipsometry (SE) [19] measurements, between 1.1 and 5.6 eV for three compositions

0953-8984/96/315757+12$19.50

($x = 0.2$, 0.5 and 0.7) at room temperature. These latter experimental data show only the transitions named E_0, $E_0 + \Delta_0$, E_1, $E_1 + \Delta_1$ and E_2 [19], but there is no evidence of e_1 and $e_1 + \Delta_1$, nor of the others near E_2. The complex dielectric function $\varepsilon = \varepsilon_r + i\varepsilon_i$ is calculated using a model dielectric function (MDF) which needs the knowledge of the energy E_ℓ, the broadening parameter Γ_ℓ and the oscillator strength A_ℓ for each critical transition ℓ. Following the results of [11] and [15] all of these necessary parameters have been interpolated linearly between their values corresponding to the end binaries CdTe and ZnTe, which have already been determined in the MDF model [20, 21]. ε calculated for $x = 0.5$ agrees reasonably with ε measured by SE. This agreement comes quite as much from the limited difference between the actual value of the parameters and the interpolated ones as from the comparison itself which is performed on ε and not on its derivatives.

This paper presents experimental results on the pseudo-dielectric function of CZT samples measured at room temperature for seven different compositions. The experimental results are analysed in the critical-point (CP) model [22]; the energies of the critical transitions and the corresponding broadening parameters are given as functions of x and discussed. The paper is organized as follows: the growth of the compounds, the surface preparation and the ellipsometric measurements are described in section 2, and the dielectric function analysis is recalled in section 3. Section 4 describes the results on the E_ℓ and Γ_ℓ. Finally section 5 gives a discussion of the results.

2. Material growth and sample surface preparation

CZT ingots were grown by the travelling-heater method (THM) using CdTe and ZnTe as source materials and Te as the solvent. The growth technique is described in great detail in [23] to which the reader is referred. The cross sections of the CdTe and ZnTe parts of the source ingot were varied along the growth axis so as to obtain a graded-composition ingot. The temperature of the hot zone was 900 °C and the growth rate 4 mm per day. The ingot was constituted of monocrystalline grains of large size ($\simeq$10 mm). Slices of 2 mm thickness and 15 mm diameter were cut with faces perpendicular to the growth axis. An x-mapping of the composition of the two faces of each slice was monitored with a microprobe [24]. Only samples where the overall deviation of x over the whole face was lower than 0.02 were kept for ellipsometric measurements. The optical elliptic spot on the sample was placed in a part where the composition gradient was the lowest but also outside the grain boundaries. We estimate that the maximum variation of x over the whole lighted area was lower than 0.002; however, the x-value is given with an uncertainty of ± 0.005. ε does not depend on the crystallographic orientation of the probed surface for cubic crystals; however, the reaction rates of the chemical reactants and the surface roughness may depend on sample crystallographic orientation which is not controlled. The binaries CdTe and ZnTe underwent a stoichiometric annealing at 750 °C under an overpressure of the metal constituent at 720 °C for 100 h to decrease the number of Te precipitates. The ternaries were not annealed as we were not able to find a reliable stoichiometric annealing for the whole composition range. The slices were mechanically polished with alumina of grain size 0.3 μm and then with alumina of grain size 0.04 μm. The slices were then chemomechanically polished with 0.5% Br_2–methanol (Br–MET). They were then ready for the last etching processes under ellipsometric control.

Ellipsometric measurements were performed with a phase-modulated spectroscopic ellipsometer UVISEL (Instrument SA) at room temperature (293 K). The ellipsometric angles ψ and Δ are defined by $r_p/r_s = \tan\psi\, e^{i\Delta}$ where r_s is the reflectivity for a polarization of the light perpendicular to the plane of incidence and r_p corresponds to a polarization

parallel to the plane of incidence. The value $\varepsilon(E)$ is easily deduced if no overlayer is considered (the two-phase model) [25].

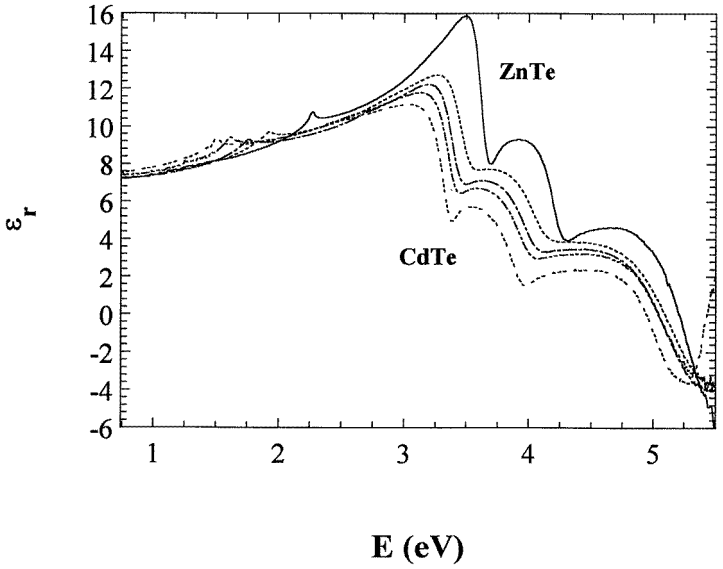

Figure 1. The real part ε_r of the dielectric function of $Cd_{1-x}Zn_xTe$ versus the photon energy E for: $x = 0$, - - - - - -; $x = 0.19$, —— - - ——; $x = 0.41$, —— - ——; $x = 0.64$, - - - -; and $x = 1$, —.

The highest value of ε_i at the E_2-peak near 5 eV was used to check the optical quality of the surface [26, 27]. This check can be performed on the ellipsometer as the sample is placed in a windowless cell under flowing argon where it can be flushed with solvents or reactants. A great number of surface treatments have been tested, especially those which have been cited in the literature on II–VI compounds for surface treatments. The highest value of $\varepsilon_i(E_2)$ was reached when the sample was freshly chemomechanically etched with 0.1% Br–MET, thoroughly rinsed with electronic-grade methanol, carried under methanol to the ellipsometer where it was mounted in the argon flow, and flushed for a final time with methanol. This result is consistent with those of Viña *et al* for HgCdTe [27] and of Sato and Adachi for ZnTe [21], who used also Br–MET. We wish to point out the importance of on using a low-concentration Br–MET solution ($\sim$0.1%). However, there is no further improvement in $\varepsilon_i(E_2)$ when using Br_2 concentrations lower than 0.1%. The $\varepsilon_i(E_2)$-value for CdTe [100] (12.15) is found to be as high as the value in red in figure 1 of [26] (12.1 to the reading accuracy). On the other hand, we found a slightly higher value of $\varepsilon_i(E_2)$ for ZnTe [100] (15.8) than that of Adachi and Kimura who give $\varepsilon_i(E_2) = 15.2$ [19]. All other processes, such as the stripping with $NaBH_4$ [28], and the neutralization with KCN [29, 30], led to lower $\varepsilon_i(E_2)$-values corresponding to the presence of an overlayer. $\varepsilon_i(E_2)$ for CdTe decreases slowly with a time constant of about 30 h to an asymptotic value 7% lower than the initial one. This decrease corresponds to an oxidation of the surface which is not fully protected from the ambient in the windowless cell. The time constant decreases with composition x and reaches 4 h for ZnTe. The overlayer can be removed after 30 h by a stripping with pure methanol as the initial $\varepsilon_i(E_2)$-value can be recovered. This overlayer is only partly removed after a long rinsing (0.5 h) in deionized water. Water removes surface oxides as for GaAs [31]; however, the remaining dissolved oxygen continues to oxidize

CZT. It is necessary to use water with a very low concentration of oxygen to achieve a nearly oxide-free surface [32].

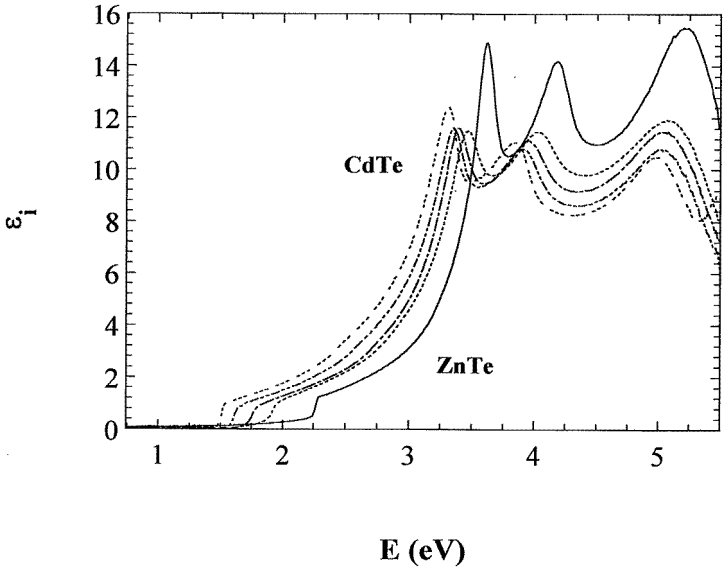

Figure 2. The imaginary part ε_i of the dielectric function of $Cd_{1-x}Zn_xTe$ versus the photon energy E for the same compositions as in figure 1.

For Zn-rich samples the surface degrades too quickly during the time of 20 minutes necessary to monitor Δ and ψ between 1.5 eV and 5.7 eV in steps of 10 meV. To overcome this difficulty, the ellipsometric data are monitored during wavelength scans which are sequentially repeated 10 to 15 times during the surface degradation [33]. The first wavelength scan is started at the photon energy E_2 when the last rinsing gives the highest value of $\varepsilon_i(E_2)$. The time of each measurement of ψ, Δ and E is referred to the starting time of the first scan. For each E-value, variations of ψ and Δ with time t, related to surface degradation, can be very well fitted with the arbitrary but simple function $r + u/(s + t)$; $r + u/s$ gives the value corresponding to the less degraded surface. This method is very time consuming but it is also an averaging procedure which increases the signal/noise ratio of the ellipsometric data. The data on the near-infrared domain (0.75 eV $< E <$ 1.5 eV) are obtained in a separate run of scans as the measurements in this spectral range require the optical fibres which link the different optical components of the ellipsometer to be changed. The sample surface is processed a further time, *in situ*, on the ellipsometer, to verify that $\varepsilon_i(E_2)$ reaches its highest value. Successive wavelength scans are then performed as previously described, the reference time being that of the maximum of $\varepsilon_i(E_2)$ just after the stripping.

3. Dielectric function analysis

The real and imaginary parts of the pseudo-dielectric function ε are deduced, for each value of E, from ψ- and Δ-values extrapolated to $t = 0$, using the two-phase model [25] in which the surface is considered perfectly flat between the bulk of the sample and the air. ε_r and ε_i are shown respectively in figure 1 and figure 2 for only five selected compositions for

clarity. ε is linked to the structure of electronic states of the ternaries which is similar to that of the end binaries. The band structure of CdTe and ZnTe has been calculated by several methods and in particular by an empirical pseudopotential method. The energy of the states is drawn for directions of high symmetry in the Brillouin zone in figure 1 of [34] for CdTe and figure 1 of [35] for ZnTe. The main interband transitions that we are concerned with in the spectral range studied are $E_0(\Gamma_8^v \rightarrow \Gamma_6^c)$, $E_0+\Delta_0(\Gamma_7^v \rightarrow \Gamma_6^c)$, $E_1(\Gamma_{4,5}^v \rightarrow L_6^c)$ or $(\Lambda_{4,5}^v \rightarrow \Lambda_6^c)$, $E_1+\Delta_1(L_6^v \rightarrow L_6^c)$ or $(\Lambda_6^v \rightarrow \Lambda_6^c)$ and E_2, including likely several transitions which appear to be separated at low temperature [34, 35] but are not definitely assigned. This broad band of the whole group of transitions has often been described with a harmonic oscillator lineshape [19, 20] but also with a one-dimensional maximum lineshape [27].

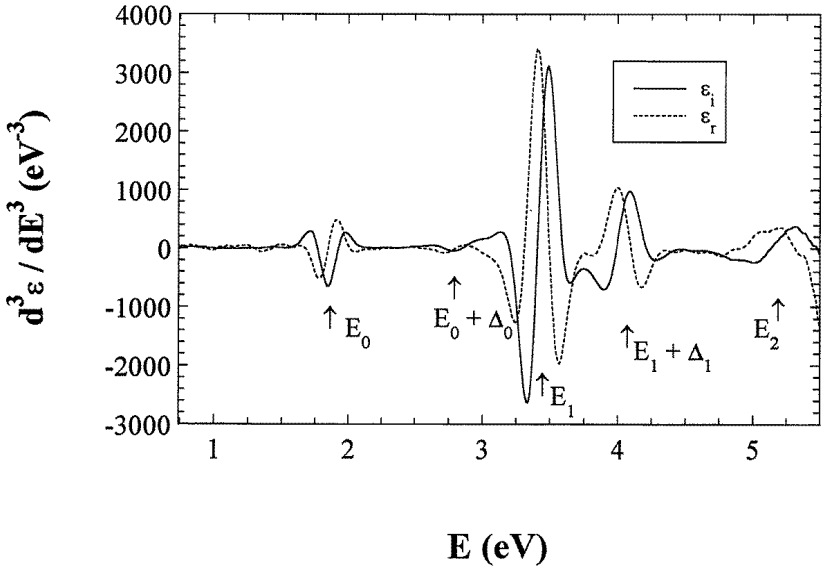

Figure 3. The third derivatives of ε_i (—) and of ε_r (- - -) for $Cd_{0.5}Zn_{0.5}Te$ versus the photon energy E. The energies of the critical transitions are indicated by arrows.

The spectral analysis of ε follows the usual CP description. The contribution around a threshold energy E_ℓ is given by the expression [22]

$$L_\ell(E) = A_\ell \Gamma_\ell^{-n} e^{i\theta_\ell}(E - E_\ell + i\Gamma_\ell)^n + F(E). \tag{1}$$

A_ℓ is the oscillator strength, Γ_ℓ the broadening parameter and n the order of the transition ($n = 1/2$ for a 3D transition, $n = 0$ (logarithmic) for a 2D transition, $n = -1/2$ for a 1D transition and $n = -1$ for a discrete exciton). $F(E)$ is a slowly varying function coming from remote transitions; its derivatives are often assumed to be negligible. θ_ℓ is a phase angle whose value is a multiple of $\pi/2$ for transitions between uncorrelated electron states. Other values of θ_ℓ represent a mixture of contiguous CPs due to excitonic effects [27, 36]. The fit of the parameters defined in (1) is performed simultaneously on the third derivatives of $\varepsilon_r(E)$ and $\varepsilon_i(E)$, which are calculated numerically from the experimental data. Statistical errors in ψ- and Δ-values extrapolated to $t = 0$ are low enough for us to obtain good results without applying any smoothing procedure. However, it is necessary to apply a slight smoothing with an exponential regression to analyse the weak transition at $E_0 + \Delta_0$. This smoothing is only applied after the calculation of the first derivative and the two next ones when it appears necessary. However, this smoothing is not applied to

Table 1. Values of the parameters a_ℓ, b_ℓ, c_ℓ deduced from the fit of critical-point energy variations with a second-order polynomial of composition x ([a] this work for E_0).

		a_ℓ	b_ℓ	c_ℓ	Error bar (meV)
E_0	[a]	1.518	0.486	0.269	±11
	[12]	1.46	0.51	0.23	
	[16]	1.51	0.606	0.139	
	[17]	1.464	0.496	0.229	
$E_0 + \Delta_0$		2.452	0.499	0.242	±24
E_1		3.362	0.028	0.242	±7
$E_1 + \Delta_1$		3.96	0.012	0.26	±9
E_2		5.04	0	0.24	±50

$\varepsilon_r(E)$ and $\varepsilon_i(E)$ as it can lead to arbitrary distortions of the lineshapes. Figure 3 gives an example of numerically calculated third derivatives; the transition energies are indicated by arrows. The fit of the parameters defined in (1) was performed with the Levenberg–Marquardt method [37]. In order to avoid the effect of possible distortions in the numerical calculations, the lineshapes described by (1) are also numerically calculated and smoothed with the same procedures as was applied to calculate the third derivatives from experimental data. This type of fit proposed by Garland *et al* [38] appears to give the most stable and reliable solutions. The same level of smoothing, when it is used, is applied to all of the fits corresponding to the same CP transition whatever the composition x is.

4. Critical-point parameters for CdZnTe

The variations of the transition energies with x are given in figure 4. They are described with quadratic laws:

$$E_\ell(x) = a_\ell + b_\ell x + c_\ell x^2 \tag{2}$$

where the values of a_ℓ, b_ℓ and c_ℓ for the different transitions are given in table 1.

The best fit of the experimental data for the E_0-transition is obtained with a 3D lineshape. The phase angle θ_0 remains around 150° when x varies; this value is higher than that of $\pi/2$ corresponding to transitions between uncorrelated states near a minimum. In return a fit with an excitonic lineshape is nearly as good as that with a 3D one. Therefore the corresponding phase angle takes values scattered over a 40° space around 290°. This mean value is far from that of a pure excitonic transition ($\theta = \pi$) and is related to a Fano profile [36, 39]. The border between excitonic transitions, clearly identified at low temperature in ZnTe and CdTe [18, 39], and transitions between weakly correlated states is probably in the vicinity of 300 K as also proposed for GaAs [39], although the binding energy of the exciton is higher in CdTe and ZnTe than in GaAs. All of the results concerning the E_0-transition are deduced from fits performed with a 3D lineshape, which leads obviously to a longer broadening parameter than with an excitonic lineshape. The transition $E_0 + \Delta_0$ is best fitted with a 3D lineshape; the phase angle for CdTe (182) and ZnTe (175) is near the value of π corresponding to an excitonic transition.

Parameter values characterizing the transitions E_1 and $E_1 + \Delta_1$ given here are obtained with a simultaneous fit of the third derivatives of the experimental data between and around

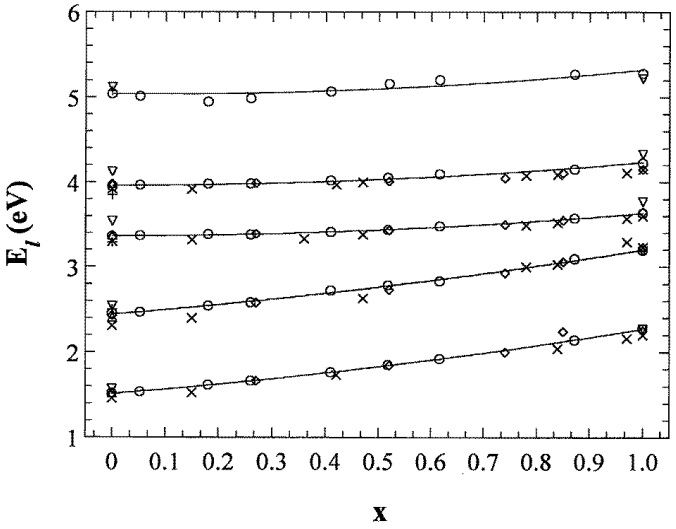

Figure 4. Experimental values of the critical transition energies E_ℓ versus composition x for $Cd_{1-x}Zn_xTe$: ○, this work; ◇, from [10]; ×, from [12]; ▽, from [20] and [21]; △, from [26]; + from [27].

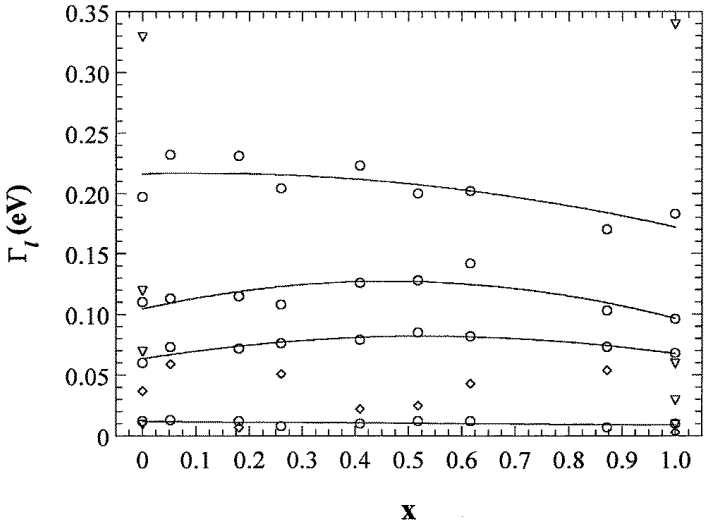

Figure 5. Experimental values of the broadening parameter Γ_ℓ versus composition x for $Cd_{1-x}Zn_xTe$: ○, this work for the transitions E_0, E_1, $E_1+\Delta_1$ and E_2; ◇, this work for $E_0+\Delta_0$; △, from [20] and [21].

E_1 and $E_1+\Delta_1$ with a 2D ($n=0$) lineshape. However, they can be fitted just as well with an excitonic lineshape ($n=-1$). The values of the parameters so deduced for ZnTe and CdTe are given in table 2. The broadening parameter needs to be larger with an excitonic lineshape than with the 2D one. The phase angles θ vary almost linearly with x between the values corresponding to the end binaries which are given in table 2 whatever lineshape is used for the fit. These monotonic variations of the phase angles express a gradual increase

Table 2. Values of the parameters defined in equation (1) for the transitions E_1 and $E_1 + \Delta_1$ in ZnTe and CdTe obtained after a fit with a 2D CP lineshape and an exciton lineshape.

	2D CP ($n = 0$)		Exciton ($n = -1$)	
	ZnTe	CdTe	ZnTe	CdTe
E_1 (eV)	3.636 ± 0.001	3.351 ± 0.002	3.629 ± 0.001	3.351 ± 0.005
θ_{E_1} (deg)	304 ± 1.5	304 ± 2	203 ± 1	215 ± 2
Γ_{E_1} (eV)	0.041 ± 0.001	0.066 ± 0.001	0.085 ± 0.001	0.113 ± 0.001
A_{E_1}	4.44 ± 0.11	3.38 ± 0.10	6.74 ± 0.06	4.04 ± 0.07
$E_1 = \Delta_1$ (eV)	4.223 ± 0.003	3.945 ± 0.005	4.221 ± 0.002	3.937 ± 0.004
$\theta_{E_1+\Delta_1}$ (deg)	311 ± 3.3	325 ± 5	219 ± 2	225 ± 4
$\Gamma_{E_1+\Delta_1}$ (eV)	0.078 ± 0.003	0.099 ± 0.003	0.138 ± 0.002	0.164 ± 0.004
$A_{E_1+\Delta_1}$	3.14 ± 0.18	2.15 ± 0.10	4.01 ± 0.1	3.93 ± 0.12

in excitonic contribution from CdTe to ZnTe.

The broadening parameters for all of the transitions are reported in figure 5. These variations are better described by an $x(1-x)$ relation than the $[x(1-x)]^{1/2}$ one which is associated with exciton broadening due to disorder. There is no effect of the atomic disorder on Γ_{E_0} as it varies linearly between the value of CdTe (12 meV) and that of ZnTe (9 meV). This is possibly also the case for $\Gamma_{E_0+\Delta_0}$ although experimental results are scattered as fits of the experimental results are not so good for this weak transition. Δ_0 and Δ_1 are given in figure 6. Their values for the end binaries agree with other determinations already given in the literature which are also reported in figure 6. Δ_0 can be considered as varying linearly with x between its values corresponding to the end binaries which are slightly different [14], whereas Δ_1 appears almost constant throughout the whole composition range. The E_2-transition is fitted with a 2D ($n = 0$) lineshape as the corresponding ε describes better a group of several transitions near the same energy [27, 36, 39].

5. Discussion of the results

The values of the transition energies for the binaries are in good agreement with those given in the literature. Some of them are reported in figure 4 together with the corresponding references. The coefficients a_ℓ, b_ℓ, c_ℓ of the quadratic law for E_0 are compared with already known results in table 1. The bowing of 0.27 eV found for E_0 at room temperature is very near to the values given for bulk compounds [10, 12, 17] but about twice that obtained for epitaxial layers [16].

To the authors' knowledge no specific calculation of the electronic structure of CZT alloys have been published. The fundamental gap variations with x can be expressed in terms of the dielectric two-band model [40]. The bowing is divided into two contributions: $C = C_i + C_d$. The intrinsic bowing C_i is obtained in the virtual-crystal approximation (VCA) assuming that the lattice constant and all other parameters vary linearly with x. The calculation gives $C_i = 0.08$ eV. The extrinsic bowing C_d is a local effect coming from the fluctuations of the potential seen by the electrons. C_d calculated with the dielectrically defined electronegativity difference between cations [41] takes a value of 0.25 eV for CdTe–ZnTe alloys. This leads to a value $C = 0.33$ eV which is a little higher than the experimental value. The broadening parameter Γ_{E_0} remains small and displays no bowing with x, showing that disorder does not affect this parameter. At room temperature the

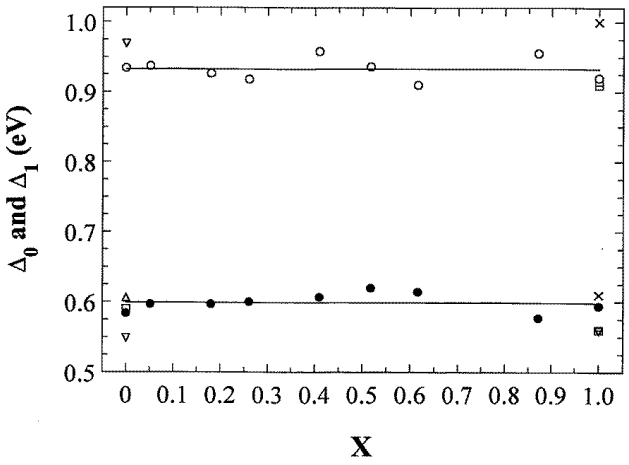

Figure 6. Experimental values of Δ_0 and Δ_1 versus the composition x for $Cd_{1-x}Zn_xTe$: ○, Δ_0 and ●, Δ_1 from this work; ×, from [12]; □, from [14]; ▽, from [20] and [21]; △, from [26]; divided square, from [48].

criterion for a negligible excitonic coupling: $\hbar\Gamma_{E_0} \gg 70E_{ex}$, where E_{ex} is the exciton binding energy whose value is around 10 meV, is far from being verified [12]. The exciton contribution remains high at this temperature, as is also indicated by the phase angle which is different from the value of $\pi/2$ corresponding to uncorrelated 3D transitions. The line broadening of the bound exciton (A^0X line) at 1.6 K increases from about 1 meV for both binaries to 11 meV near $x = 0.7$ [42]. The increase in line broadening with alloying is a consequence of the statistical fluctuations in the local concentrations of the cations Cd or Zn. Such an increase in Γ_{E_0} is not found here and demonstrates that the thermal energy at 300 K is high enough to suppress localization effects. The broadening of the electronic states in the alloy [43] gives another contribution to Γ_{E_0}; our results show that it is very weak in CdZnTe. The spin–orbit splittings in the valence band, Δ_0 and Δ_1 (cf. figure 6), do not present a significant bowing. This behaviour is found for Δ_0 for HgZnTe [33] and probably for HgCdTe; on the other hand Δ_1 has a quadratic variation with composition in a great number of III–V and II–VI alloys [27, 44].

An estimation of the bowing of Δ_0 made using the heuristic model of Van Vechten *et al* [44] leads to a value of 4.5 meV which cannot be established with the determination accuracy of Δ_0. The Δ_0-bowing can be also estimated in the tight-binding approximation as was done recently for II–VI binary compounds [45]. $\Delta_0 = a^2\Delta(\mathrm{VI}) + b^2\Delta(\mathrm{II})$ where $\Delta(\mathrm{VI})$ and $\Delta(\mathrm{II})$ are properly renormalized spin–orbit splittings for the cation (II) and the anion (VI) [46], $a^2 + b^2 = 1$ and [47]

$$\frac{\alpha}{\beta} = \frac{-2V}{E_p^{VI} - E_p^{II} + [(E_p^{VI} - E_p^{II})^2 + 4V^2]^{1/2}}.$$

Here E_p^{VI} and E_p^{II} are the energies of the atomic p states of the VI and II elements, and V are the matrix elements connecting p states of nearest neighbours separated by the distance d. $V = 12.8/d^2$ (in eV Å^{-2}) gives a good approximation of this matrix element. E_p^{II} has the same value (3.38 eV) for Zn and Cd [47] and α/β depends only on $V \propto 1/d^2$. V is calculated assuming that d is the same for the Zn–Te an Cd–Te bonds. Then, the variation of Δ_0 is scaled to the experimental values of ZnTe and CdTe rather than the calculated ones [45] for which the difference between the values of Δ_0 is lower. The calculation gives a

bowing parameter of 6 meV which cannot be demonstrated experimentally. In CZT the distribution of nearest-neighbour distances is bimodal [48]; however, a linear mixing of the values of α and β calculated with the actual Zn–Te and Cd–Te distances for $x = 0.5$ leads practically to the same value of the bowing parameter. A linear variation of Δ_0 with x gives thus a good approximation to the spin–orbit splitting at Γ. Our values of Δ_0 agree well with that of 0.91 eV found for $x = 0.2$ [49] as deduced from photoelectron emission spectroscopy experiments, which show however a strong bowing in the width of this split-off band [49]. The bowing of Δ_0 is also evaluated on the basis of the phenomenological description given in [43]. This leads to a low negative bowing of about 15 meV which appears difficult to establish from experimental data.

The departure of E_1 and $E_1 + \Delta_1$ from the linear variation between the values for the binaries is symmetric (cf. figure 5) and is well described by an $x(1 - x)$ relation. This behaviour is like those found for a great number of ternary compounds. It is different from those found for HgCdTe [27] where the deviation from linearity is at its maximum for $x \simeq 0.8$ and for HgZnTe where the maximum is near $x \simeq 0.55$ [33]. The asymmetry in the variations of E_1 and $E_1 + \Delta_1$ must be due therefore to Hg atomic levels and not to the bimodal distribution of near neighbours in HgZnTe and HgCdTe.

The quadratic expression (2) does not describe properly the variations of E_2 with composition. In fact $E_2(x)$ has an S shape with a minimum near $x = 0.2$ which is not clearly visible in figure 4. Reflectivity [10, 11] and absorption spectra [13] display shoulders near 5 eV which are assigned to the $E_0(\Gamma_8^v \rightarrow \Gamma_7^c)$ transition. These shoulders are seen in reflectivity curves at 15 K for the binaries CdTe [34] and ZnTe [35] and also at 77 K [50]. For ZnTe, the shoulder remains weak at room temperature in [35] but is not visible in the reflectivity spectra of [50]. This shoulder is disappearing for CdTe at 300 K [50]. Room temperature ellipsometric measurements on CdTe [20] and ZnTe [21] have not revealed a singularity below the E_2-transition in the vicinity of 5 eV. The E_0-transition merges probably in the low-energy part of the E_2-peak; it decreases in energy and amplitude when x increases [43, 10]. This leads probably to the nonmonotonic variation of the energy E_2. This hypothesis can also explain the relatively large scatter in values of Γ_{E_2}. The bowing for all of the critical transition energies is around 0.25 eV which leads to shifts of about 60 meV for $x = 0.5$ with regard to linear interpolations. This linear interpolation scheme used by Adachi and Kimura [19] for all of the parameters defining the critical transitions appears to be a crude approximation. ε_r and ε_i so calculated and with the MDF model do not reproduce well the experimental results for $x = 0.5$ (see figure 8 of [12]). A comparison of calculated and experimental derivatives of ε_r and ε_i shows better the differences due to the linear description of E_ℓ, Γ_ℓ and A_ℓ.

Finally we want to stress that the optical dielectric response of CZT does not show any significant behaviour which can be related to clustering effects or bond strengthening between $x = 0$ and $x = 0.1$ as evident from the vibrations of cation atoms [51]. Likewise there is no evidence of a ferroelectric transition when the Curie temperature in CZT has been found above room temperature for $x > 0.04$ [52].

6. Summary

The dielectric response measured by spectroscopic ellipsometry for CdZnTe solid solutions is given for the first time for the whole composition range. The dielectric function is analysed with the critical-point model and the parameters associated with each critical transition are given and discussed.

References

[1] Quadri S B, Skelton E F, Webb A W and Kennedy J J 1985 *Appl. Phys. Lett.* **46** 257
[2] Kennedy J J, Amirtharaj P M, Boyd P R, Quadri S B, Dobboyn R C and Long G G 1988 *J. Cryst. Growth* **86** 93
[3] Bruder M, Figgemeier H, Schmitt R and Maier H 1993 *Mater. Sci. Eng.* B **16** 40
[4] Hirata K and Oda O 1986 *Mater. Lett.* **5** 42
[5] Scharager C, Siffert P, Holtzer A and Schieber M 1980 *IEEE Trans. Nucl. Sci.* **27** 276
[6] Lambert B, Gauneau M, Grandpierre G, Schoisswohl M, Von Bardeleben H J, Launay J C, Mazoyer V, Aoudia A, Rzepka E, Marfaing Y and Triboulet R 1995 *Opt. Mater.* **4** 267
[7] Sugiyama I, Hobbs A, Saito T, Veda O, Shinohara K and Takigawa H 1992 *J. Cryst. Growth* **117** 161
[8] Tuffigo H, Magnea N, Mariette H, Wasiela A and Merle d'Aubigne Y 1991 *Phys. Rev.* B **43** 14 629
[9] Cibert J, Andre R, Deshayes C, Dang Le Si, Okumura H, Tatarenko S, Feuillet G, Jouneau P H, Mallard R and Saminadayar K 1992 *J. Cryst. Growth* **117** 424
[10] Saito K, Ebina A and Takahashi T 1972 *Solid State Commun.* **11** 841
[11] Sredin V G, Pashkovskii M V, Vasilina Z S and Evstigneev A I 1974 *Sov. Phys.–Semicond.* **7** 1566
[12] Tyagai V A, Snitko O V, Bondarenko V N, Vitrikhorskii N I, Popov V B and Krasiko A N 1974 *Sov. Phys.–Solid State* **16** 885
[13] Sredin V G 1978 *Sov. Phys.–Semicond.* **12** 1084
[14] Nimtz G 1982 *Landolt–Börnstein Numerical Data. The Physics of II–VI and I–VII Compounds* vol 17b (Berlin: Springer) p 247
[15] Kroitoru S G, Maksimova Q G and Sobolev V V 1975 *Sov. Phys.–Semicond.* **9** 1191
[16] Olego D J, Faurie J P, Sivananthan S and Raccah P M 1985 *Appl. Phys. Lett.* **47** 1172
[17] Johnson S M, Sen S, Honkel W H and Kalisher M H 1991 *J. Vac. Sci. Technol.* B **9** 1897
[18] Granger R 1994 Properties of narrow gap cadmium based compounds *EMIS Data Review 10* ed P Capper, p 429
[19] Adachi S and Kimura T 1993 *Japan. J. Appl. Phys.* **32** 3496
[20] Adachi S, Kimura T and Suzuki N 1993 *J. Appl. Phys.* **74** 3435
[21] Sato K and Adachi S 1993 *J. Appl. Phys.* **73** 926
[22] Aspnes D E 1980 *Handbook on Semiconductors* vol 2, ed M Balkanski (Amsterdam: North-Holland)
[23] Triboulet R, Neu G and Fotouhi B 1983 *J. Cryst. Growth* **65** 262
[24] West Micropobe Facility IFREMER, Brest, France
[25] Azzam R M and Bashara N M A 1987 *Ellipsometry and Polarized Light* (Amsterdam: North-Holland)
[26] Arwin H and Aspnes D E 1984 *J. Vac. Sci. Technol.* A **2** 1316
[27] Viña L, Umbach C, Cardona M and Vodopyanov L 1984 *Phys. Rev.* B **29** 6752
[28] Aspnes D E and Arwin H 1984 *J. Vac. Sci. Technol.* A **2** 1309
[29] Tene R, Brener R and Triboulet R 1989 *J. Vac. Sci. Technol.* A **7** 2570
[30] Quemerais A, Khelladi K H, Lemoine D, Granger R and Triboulet R 1994 *J. Cryst. Growth* **138** 934
[31] Massies J and Contour J P 1985 *J. Appl. Phys.* **58** 806
[32] Hirota Y 1994 *J. Appl. Phys.* **75** 1798
[33] Castaing O, Benhlal J T, Granger R and Triboulet R 1996 *J. Physique* I **6** 907
[34] Chadi D J, Walter J P, Cohen H L, Petroff Y and Balkanski M 1972 *Phys. Rev.* B **5** 3058
[35] Walter J P, Cohen M L, Petroff Y and Balkanski M 1970 *Phys. Rev.* B **1** 2661
[36] Cardona M 1966 Modulation spectroscopy *Solid State Physics* Suppl 11, ed F Seitz, D Turnbull and H Ehrenreich (New York: Academic)
[37] Press W H, Flannery B P, Tenkolsky S A and Vetterling W T 1989 *Numerical Recipes, the Art of Scientific Computing* (Cambridge: Cambridge University Press) p 523
[38] Garland J W, Kim C C, Abad H and Raccah P M 1993 *Thin Solid Films* **233** 148
[39] Lautenschlager P, Garriga M, Logothetidis S and Cardona M 1987 *Phys. Rev.* B **35** 9174
[40] Gross E F, Grigorovich G M, Pozdnyakov I V, Sredin V G and Suslina L G 1971 *Sov. Phys.–Solid State* **12** 2352
[41] Van Vechten J A and Bergerstresser T K 1970 *Phys. Rev.* B **1** 3351
[42] Oettinger K, Hofmann D M, Efros Al L, Meyer B K, Salk M and Benz K W 1992 *J. Appl. Phys.* **71** 4523
[43] Hass K C, Ehrenreich H and Velicky B 1983 *Phys. Rev.* B **27** 1088
[44] Van Vechten J A, Berolo O and Wooley J C 1972 *Phys. Rev. Lett.* **29** 1400
[45] Willatzen M, Cardona M and Christensen N E 1995 *Phys. Rev.* B **51** 17 992
[46] Chadi D J 1977 *Phys. Rev.* B **16** 790
[47] Harrison W A 1980 *Electronic Structure and the Properties of Solids* (San Francisco, CA: Freeman)

[48] Motta N, Balzarotti A, Letardi P, Kisiel A, Czyzyk M T, Zimnal-Starnawska M and Podgorny M 1985 *Solid State Commun.* **53** 509
[49] Niles D W and Hochst H 1992 *Phys. Rev.* B **46** 1498
[50] Cardona M and Greenaway D L 1963 *Phys. Rev.* **131** 98
[51] Comedi D, Kalish R and Richter V 1988 *Phys. Rev. Lett.* **61** 2125
[52] Weil R, Nkum R, Muranevich E and Benguigui L 1989 *Phys. Rev. Lett.* **62** 2744